Final Report

DEVELOPMENT OF A Ti:Al_2O_3 LASER FOR REMOTE SENSING OF THE ATMOSPHERE

Order # L-67752D
ODURF # 180590

Dr. Hani Elsayed-Ali
Professor
Department of Electrical and Computer Engineering
Old Dominion University
Norfolk, VA 23529-0246

May 1998

NASA Contact

Dr. Russell J. Deyoung
Mail Stop 401A
Atmospheric Sciences Division
NASA Langley Research Center
Hampton, VA 23681-0001

During the past year, the following research has been conducted on the Titanium Sapphire Laser system development project.

1. Characterization of the laser system.

Some characterizations of the laser system have been done. As shown in Figure 1. The temporal current profile is measured against the input energy. The typical pulse width is 5-7 microseconds. Figure 2 shows the rod fluorescence versus input energy. Also, the spatial profile of the flashlamp light distribution is measured, and the resulting distribution is close to an ellipse distribution.

2. The Gain Measurements

The gain profile measurement helps to investigate optical properties of the pump cavity as well as relative importance of various absorption transitions in the optical pumping process. Measurement of the small signal gain of the Ti:Sapphire rod is important for the modeling of Ti:Sapphire laser performance.

An 820-nm diode laser beam, (SONY SLD-304XT-1, maximum output 1W), is injected into the laser rod, and detected by a diode detector. The output is recorded on a digital oscilloscope. In order to reduce the interference from the flashlamp pulse and Ti:Sapphire rod fluorescence, the output signal is reflected with the help of a mirror next

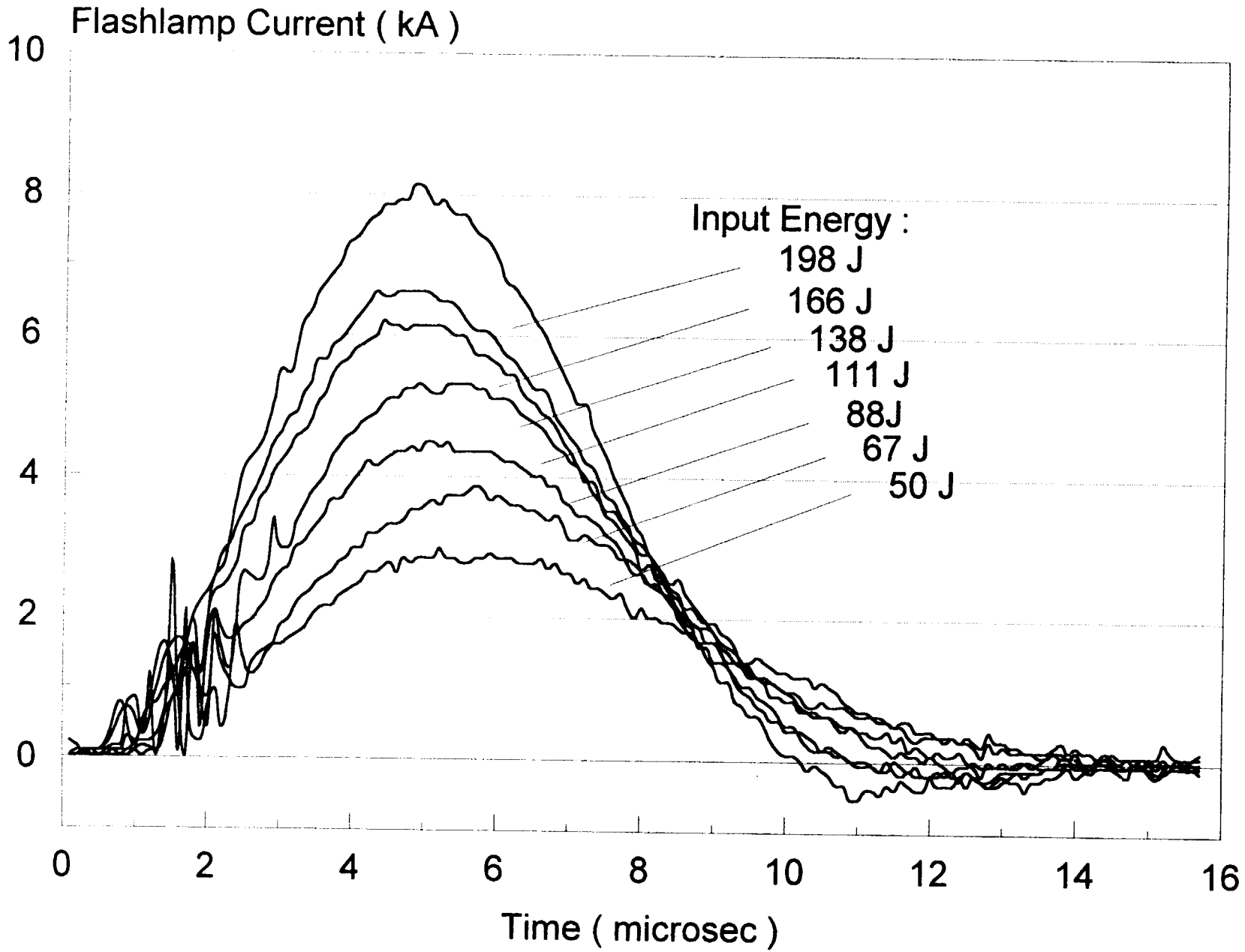

Figure 1. Current versus input energy.

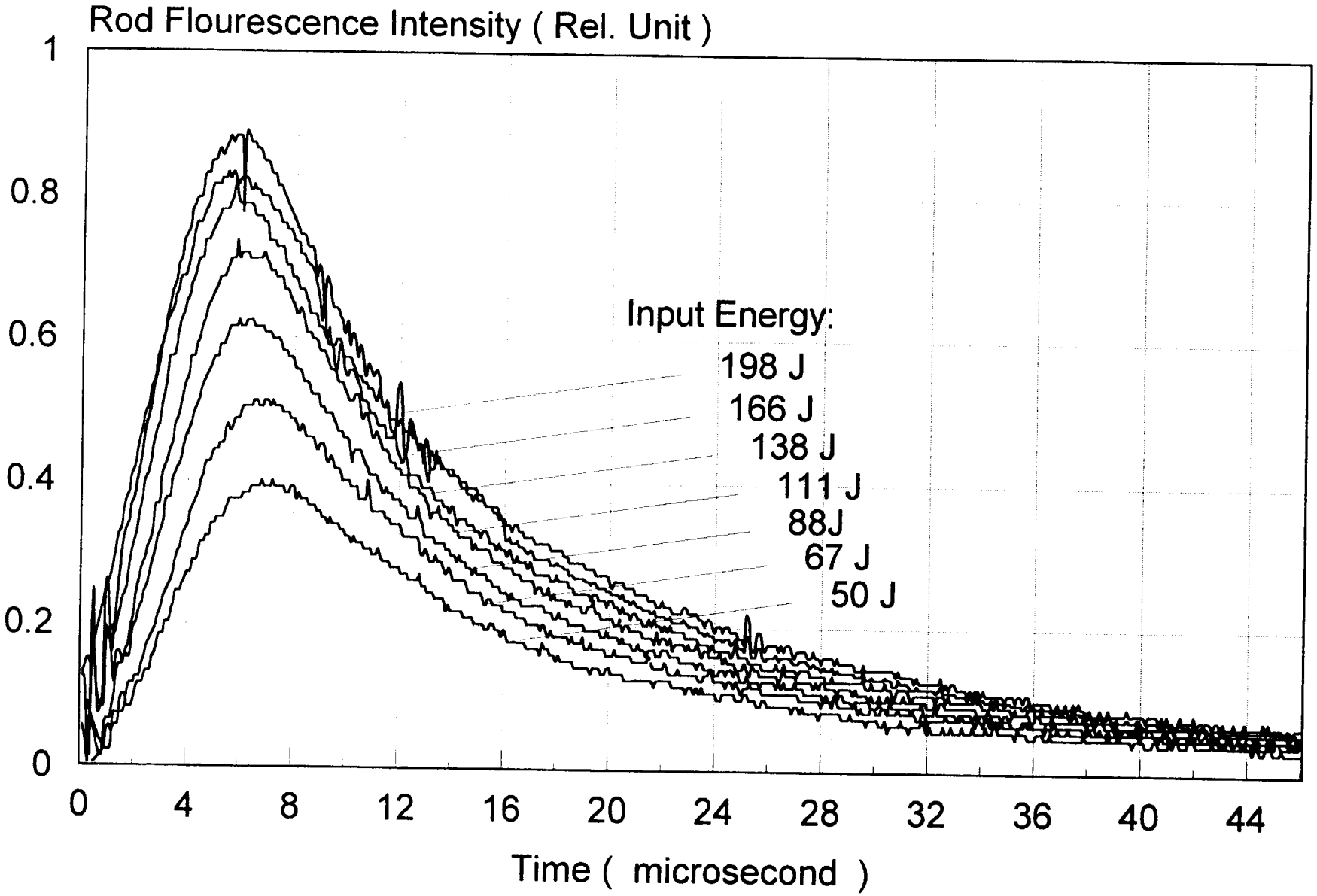

Figure 2. Rod flourescence versus input energy.

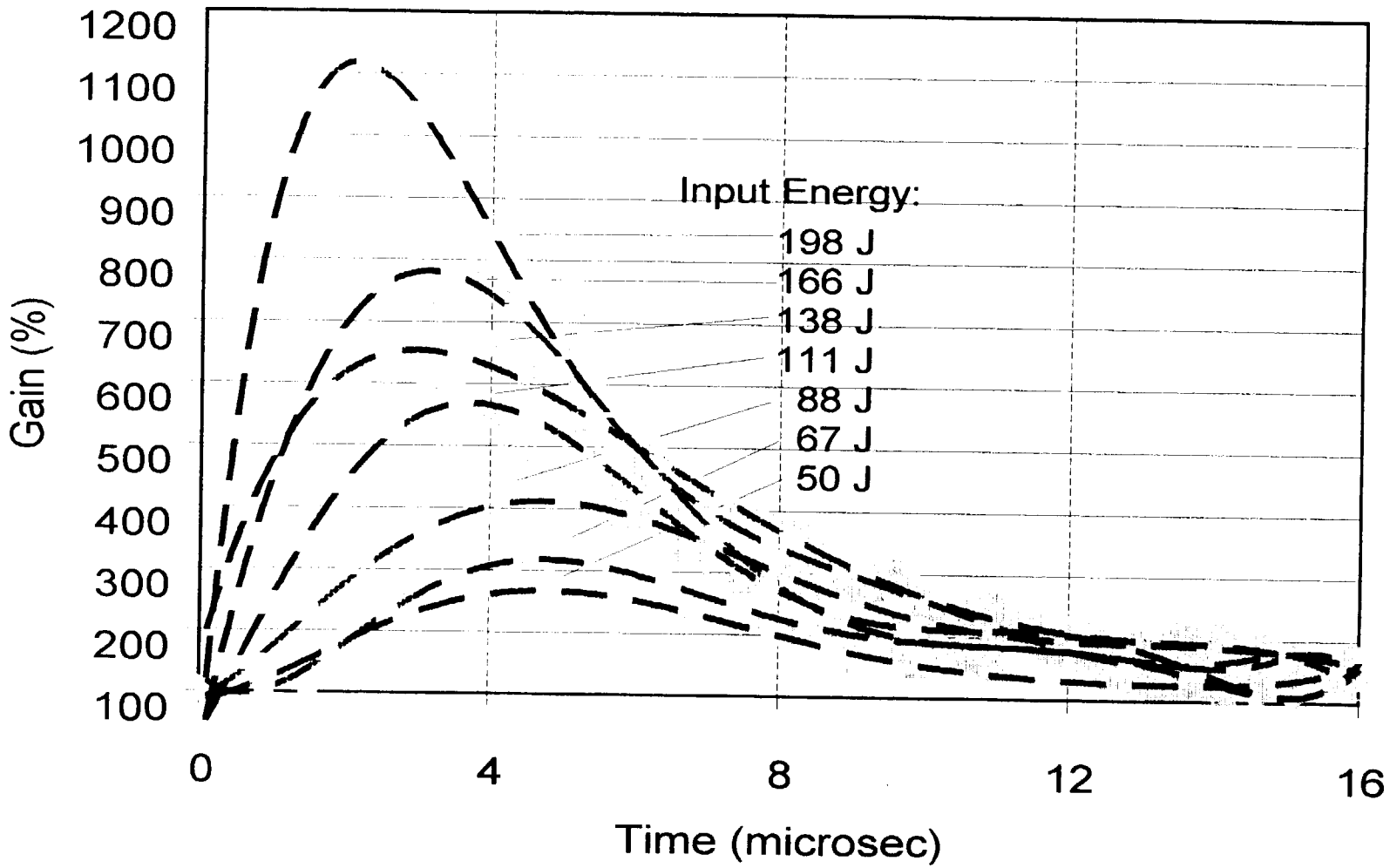

Figure 3. Laser small gain versus input energy.

divergence, high radiance (W/cm^2), and short in time. A telescope system is used to reduce the beam size from the output of the laser to fit into the harmonic generation crystal. Figure 4 shows the measuered linewidth of 867 nm output with a very small aperture, but the output energy is hampered at the aperture. Figure 5 shows the linewidth of 867 nm output without etalon. And figure 6 shows the linewidth of 867 nm output with etalon. Without much loss, the etalon helps bring down the linewidth to a significant amount.

4. Laser temporal result

Figure 7 shows temporal characteristics of flashlamp pulse, gain, and Q-switch laser output. It is noticeable that the laser gain is following the input flashlamp pulse closely.

Figure 8 shows temporal profile of THG 289 nm output. The linewidth in time is reduced compared to the fundamental, probably due to the fact that only part of the fundamental which is high Watt per Centimeter Square could produced the harmonic generation.

Figure 9 shows the output energy of 289 nm versus the fundamental energy.

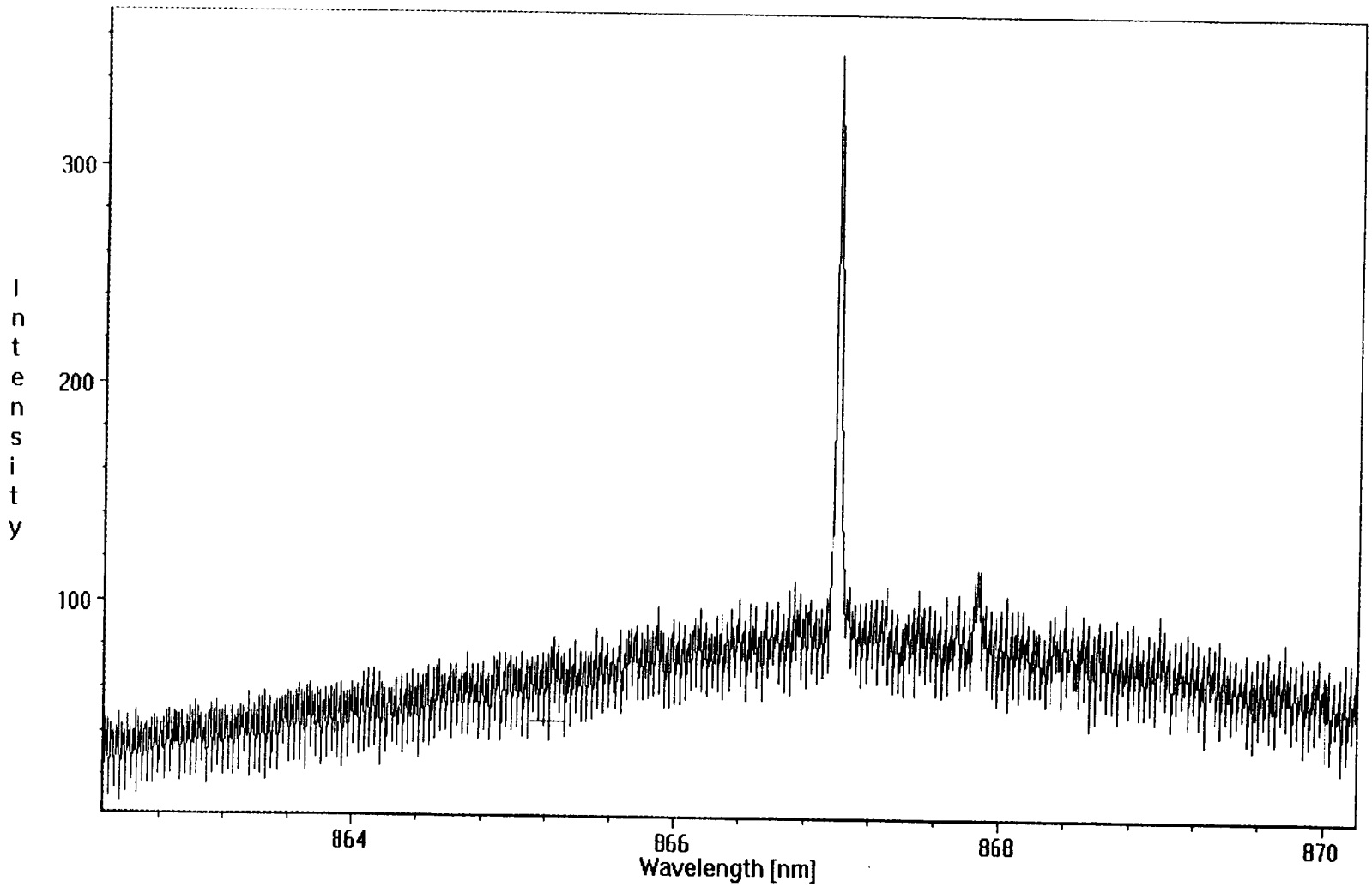

Figure 4. Linewidth of 867 nm output.

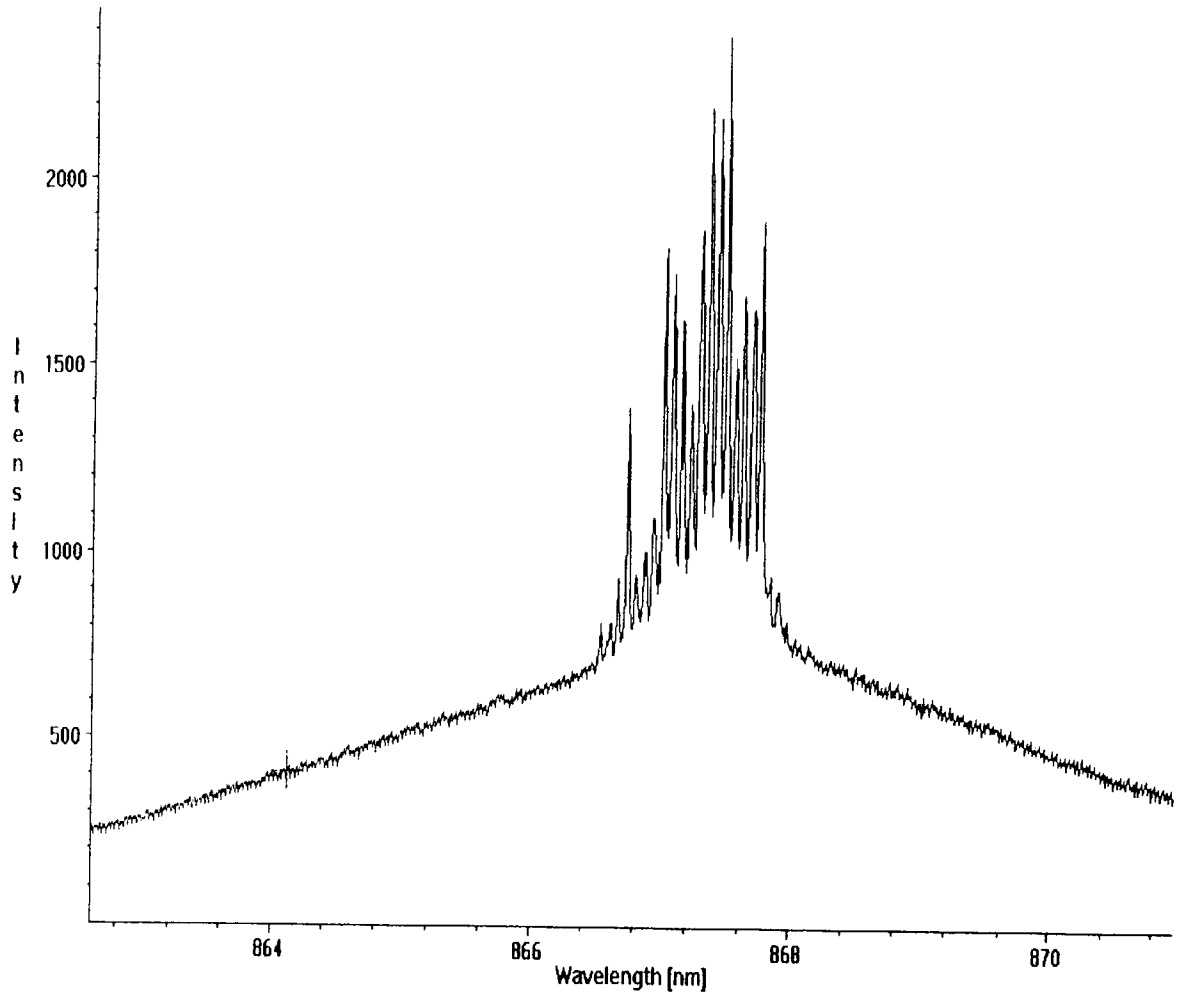

Figure 5. Linewidth of 867 nm output without etalon.

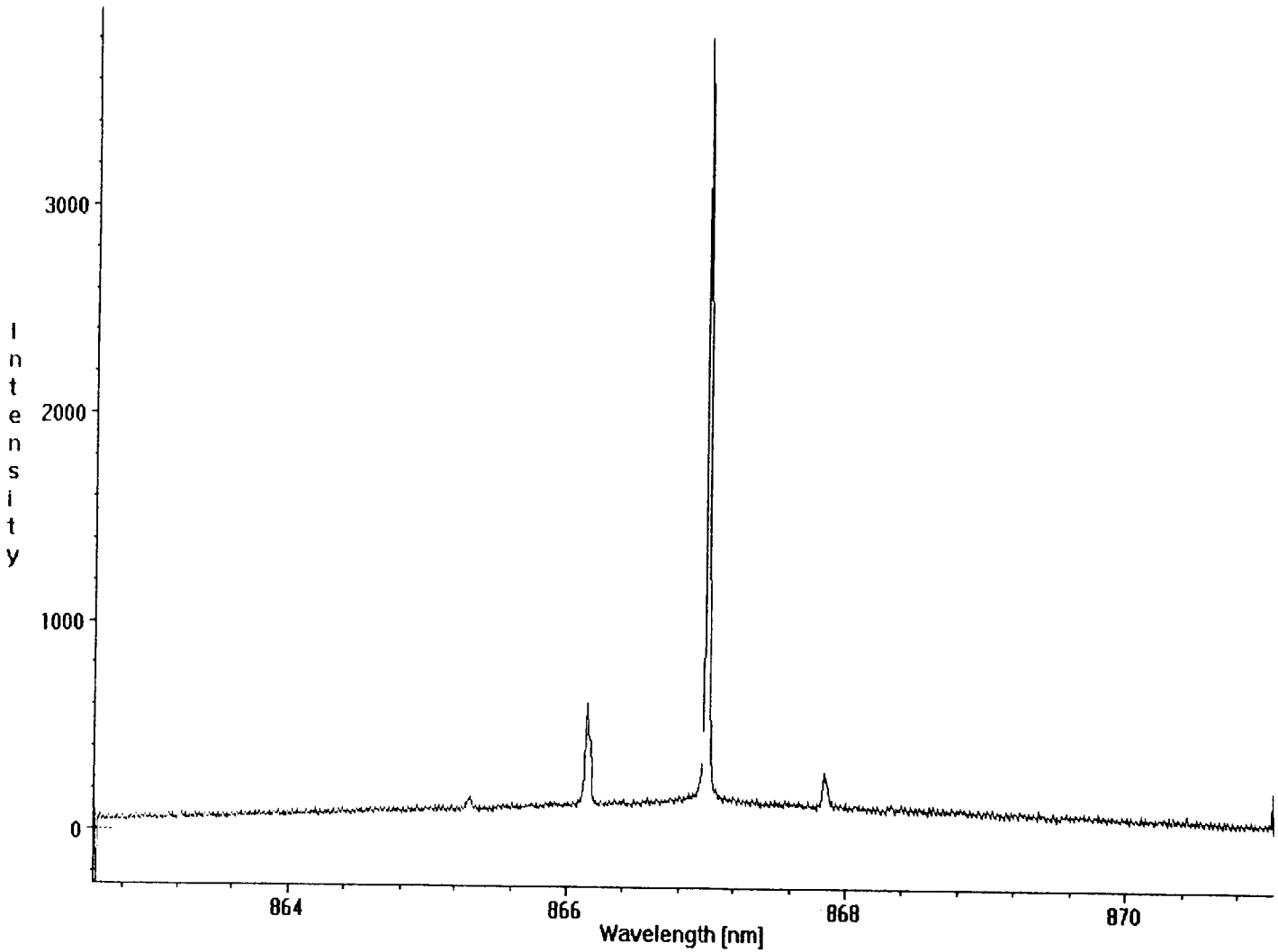

Figure 6. Linewidth of 867 nm output with etalon.

Figure 10 shows second and third harmonic generation output versus fundamental energy (867 nm). Figure 11 shows the second and third harmonic generation output versus fundamental energy (867 nm). The result indicates that there is a slight increase in output energy thanks to having the etalon. The SHG conversion efficiency is measured to be 5%. By calculating the watt per Centimeter Square, the theoretical SHG efficiency is 10% which is slightly higher that the experimental result.

Figure 12. shows the second and third harmonic generation output versus fundamental energy (897 nm) in a similar fashion. Due to the lower gain of the 897 nm branch and lower resulting watt per centimeter square, the output from 299 nm is much lower that the counter part in 289 nm.

5. Laser modeling result

Some laser modeling effort has been made. A rate equation laser model is built. Figure 13 shows the output from the laser model with 140 J input Energy, and figure 14 show the output from the laser model with 180 J input Energy.

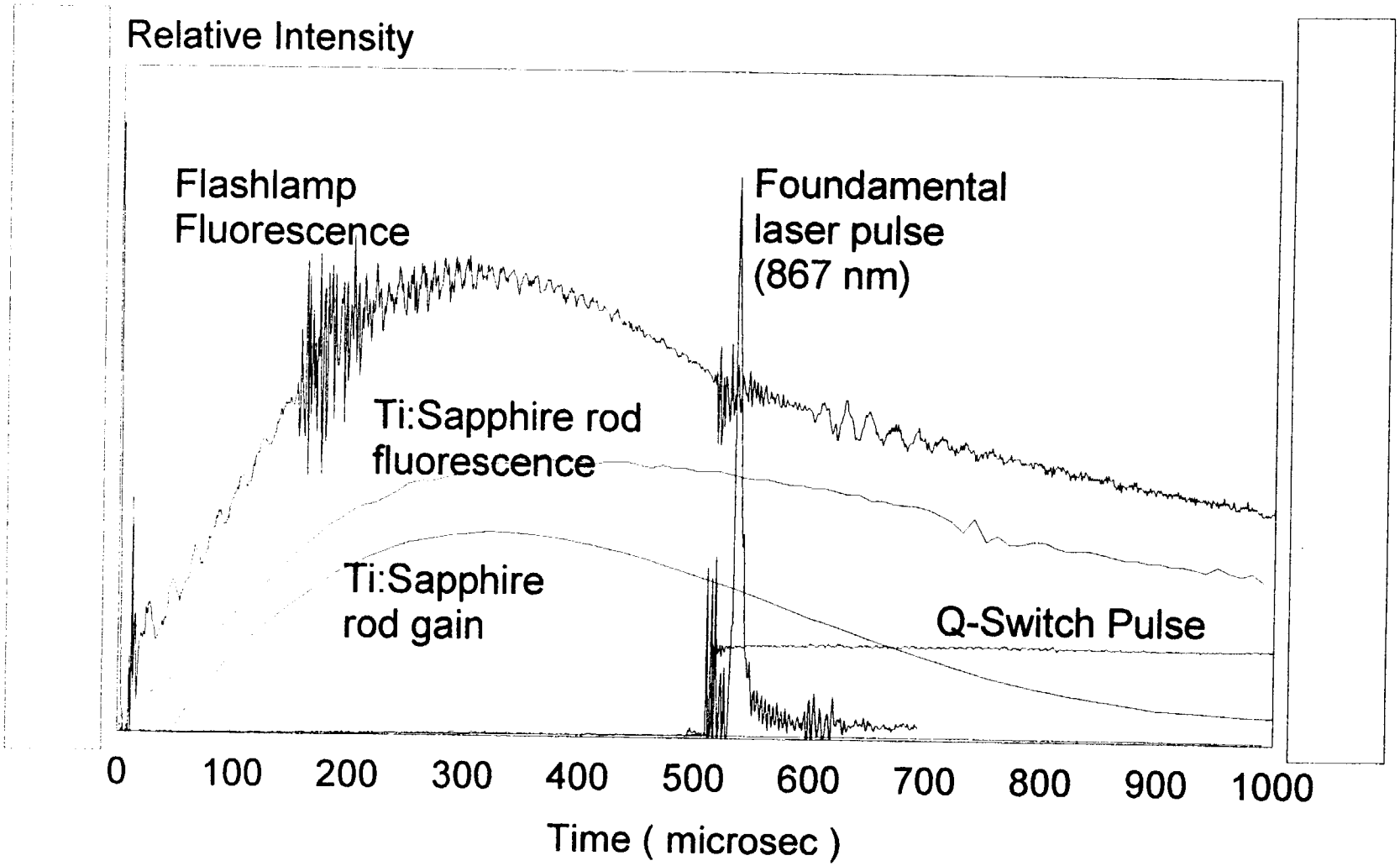

Figure 7. Temporal characteristics of flashlamp pulse, gain, and Q-switch laser output.

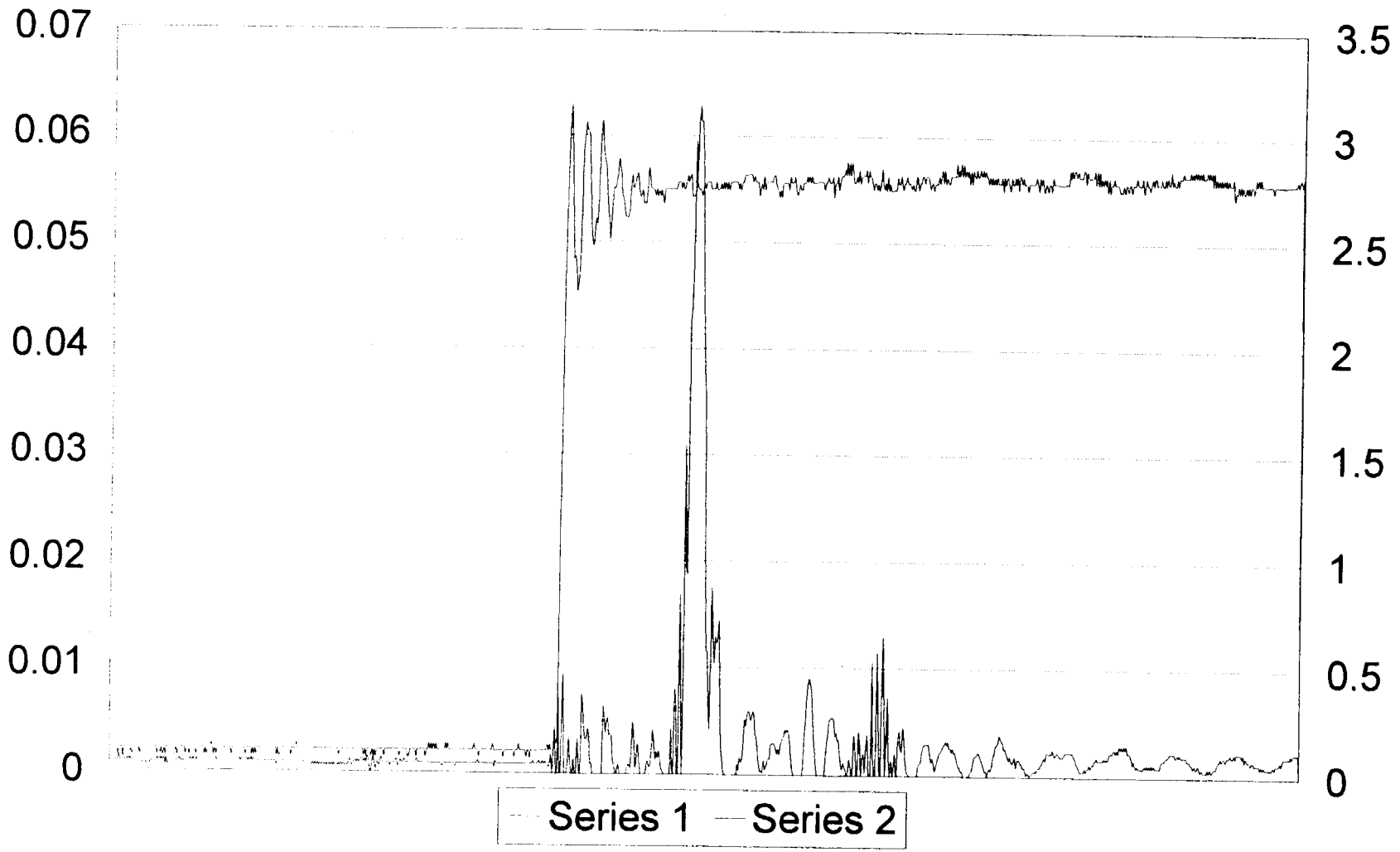

Figure 8. Temporal profile of THG 289 nm output.

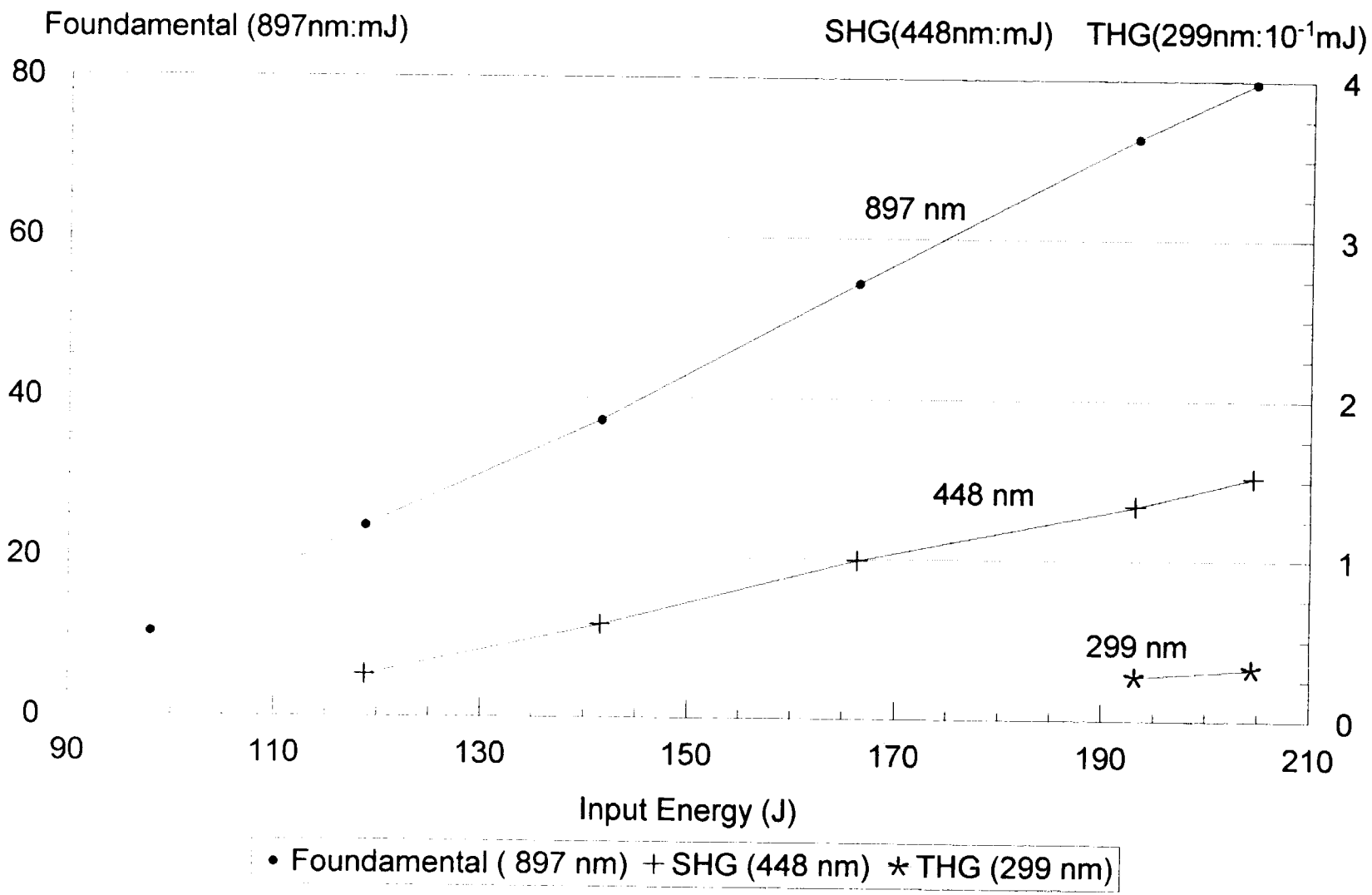

Figure 9. Output energy of 289 nm versus the fundamental energy.

to the laser head, and lead to a distance from the flashlamps so as to reduce the interference from the flashlamps, the residue portion of the flashlamp signal is subtracted from the total detector signal. Then the output signal with and without any flashlamp pumping are compared to determine the net gain from a function of flashlamp energy. Figure 3 shows the laser small gain versus input energy. The maximum gain measured is about 11 times the input.

3. Second and third harmonic generation

The fundamental laser output from the GRM at the 867-nm and 897-nm branch are converted to the UV by second and third harmonic generation. An LBO (Lithium Boronide) crystals were chosen for second harmonic generation based on the wide angular acceptance, high damage threshold, and relatively high conversion efficiency at the fundamental wavelength. The BBO (Barium Boronide) was chosen for third harmonic generation, based on the high conversion efficiency[6]. The dimension of the LBO is 3x3x12 mm, for BBO it is 3x3x7 mm. Angular tuning is employed for the harmonic generation. Type I conversion is used for SHG and Type II conversion is used for THG. Both the crystals are AR coated, and manufactured by CASIX, Inc.

In order to achieve higher second and third harmonic generation, the output beam of the fundamental laser beam should be of high beam quality (Gaussian beams), low

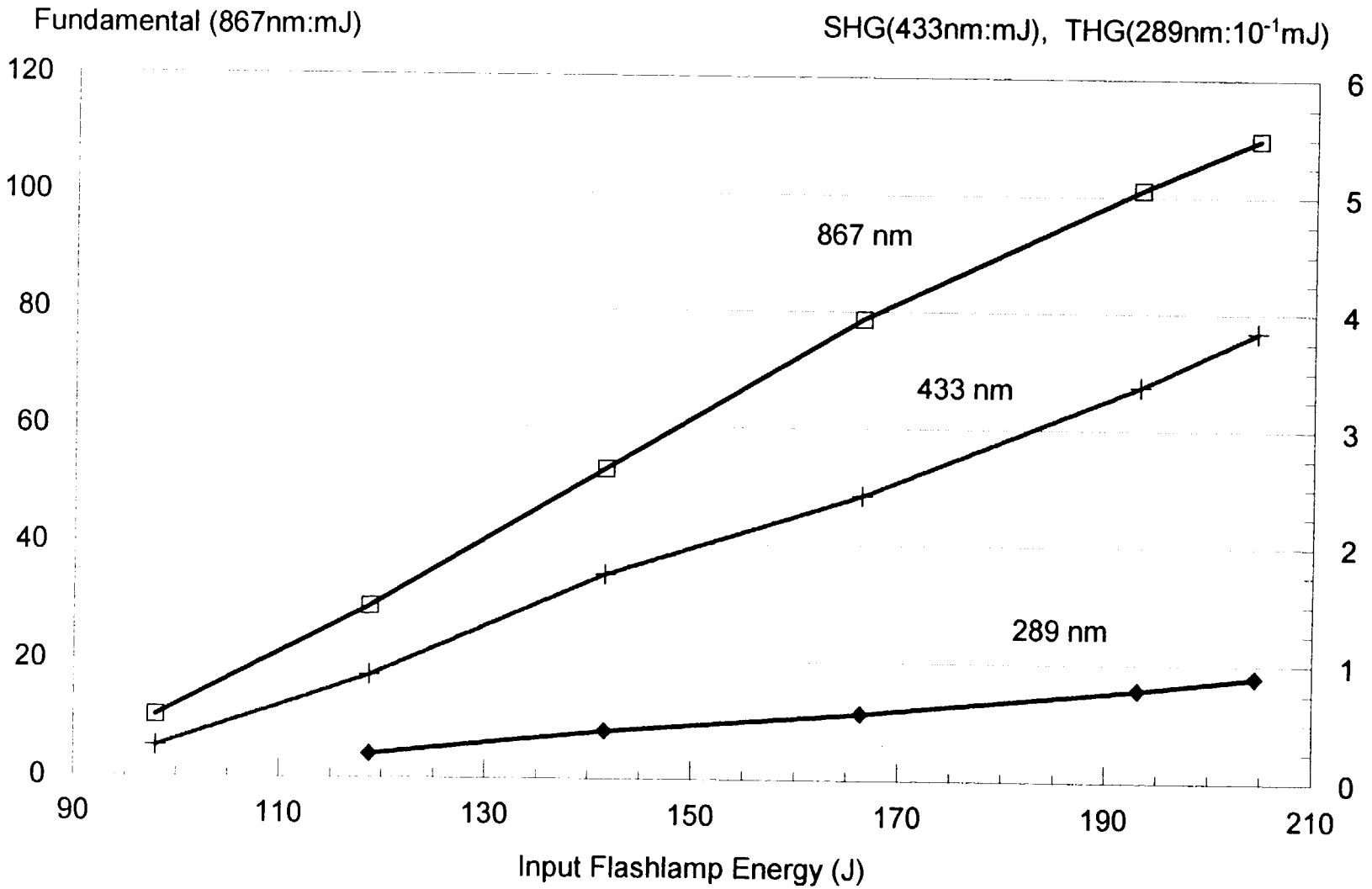

Figure 10. Second and third harmonic generation output versus fundamental energy (867 nm).

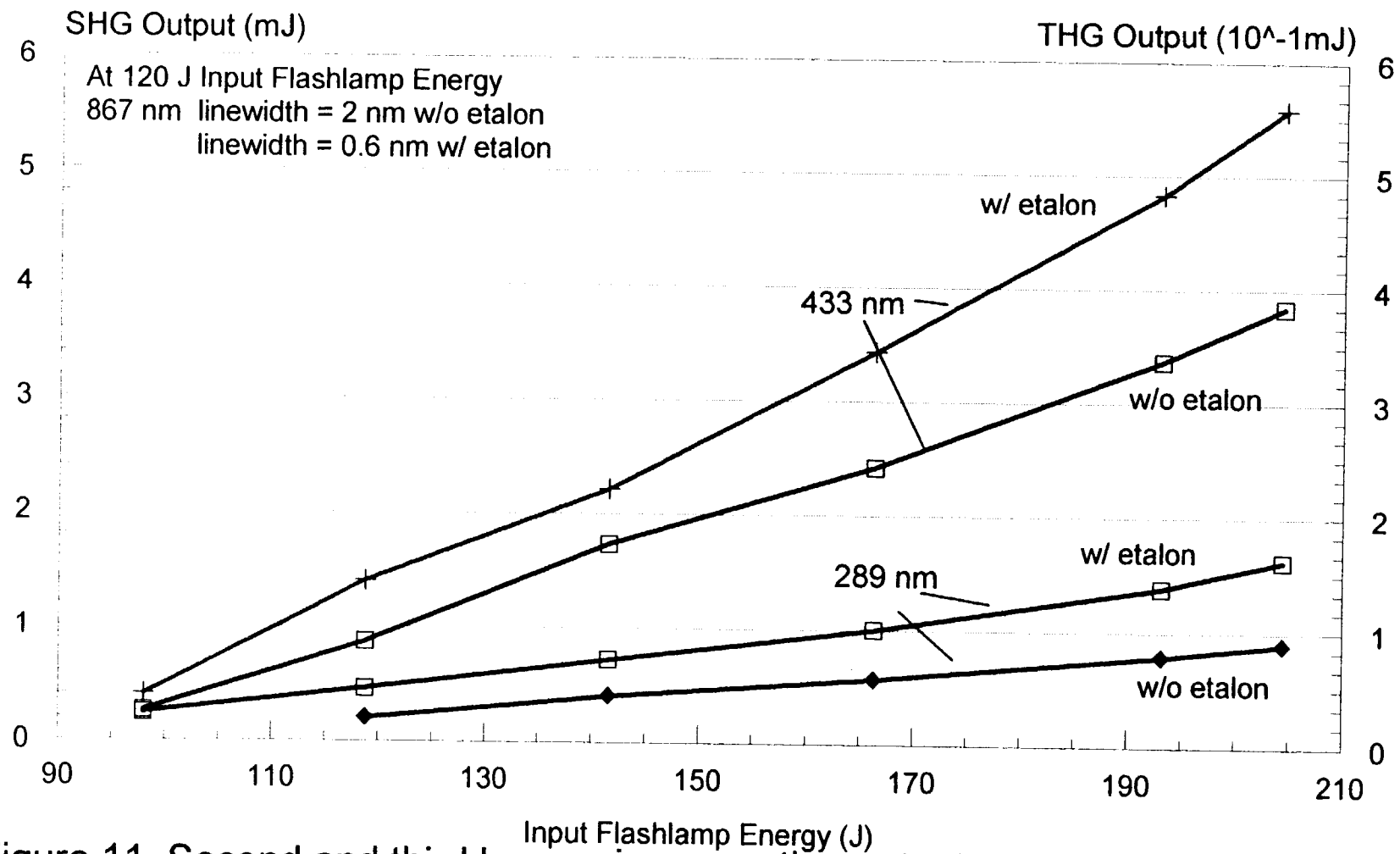

Figure 11. Second and third harmonic generation output versus fundamental energy (nm). SHG and THG with and without Etalon in the Cavity

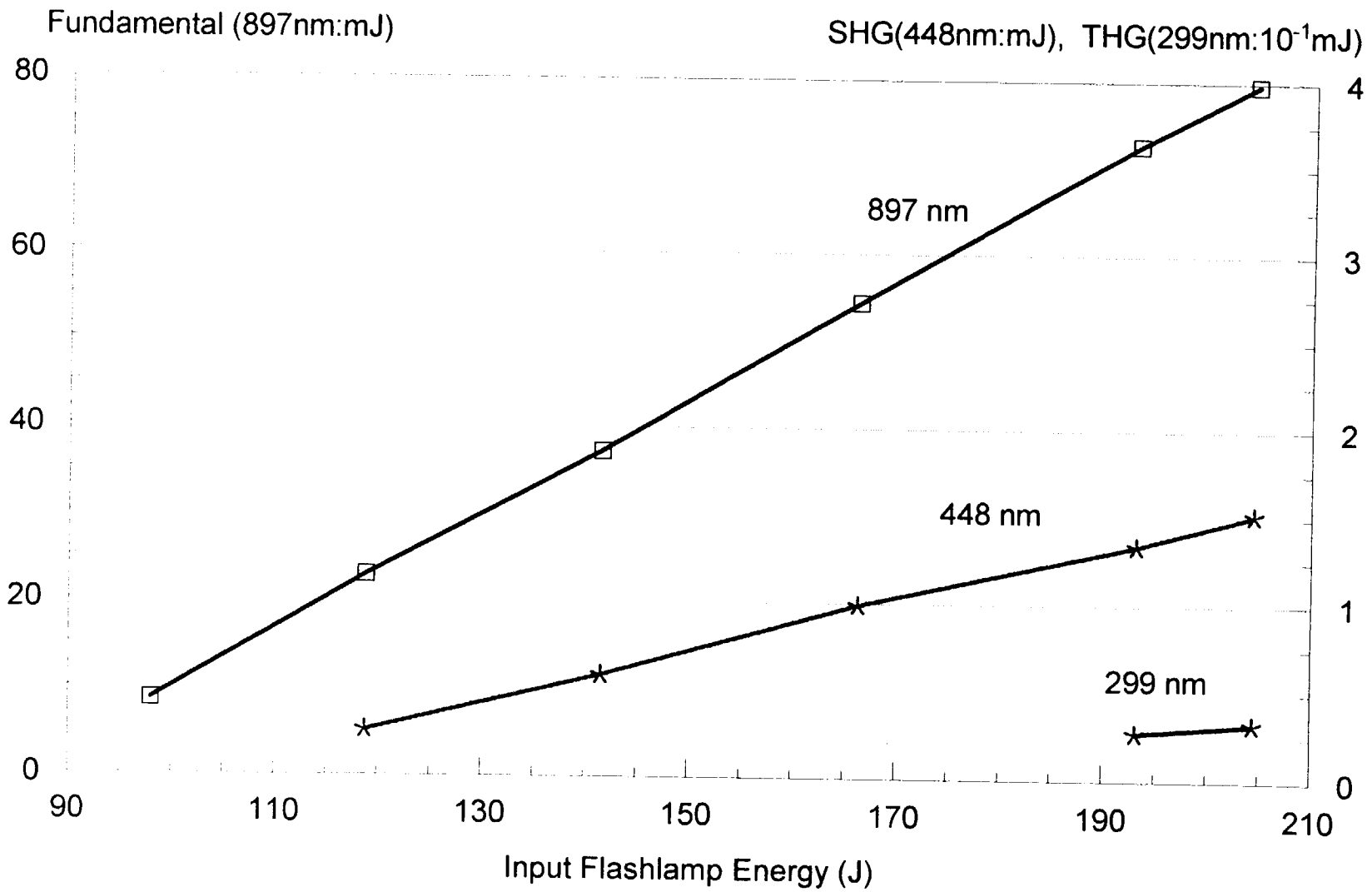

Figure 12. Second and third harmonic generation output versus fundamental energy (897 nm).

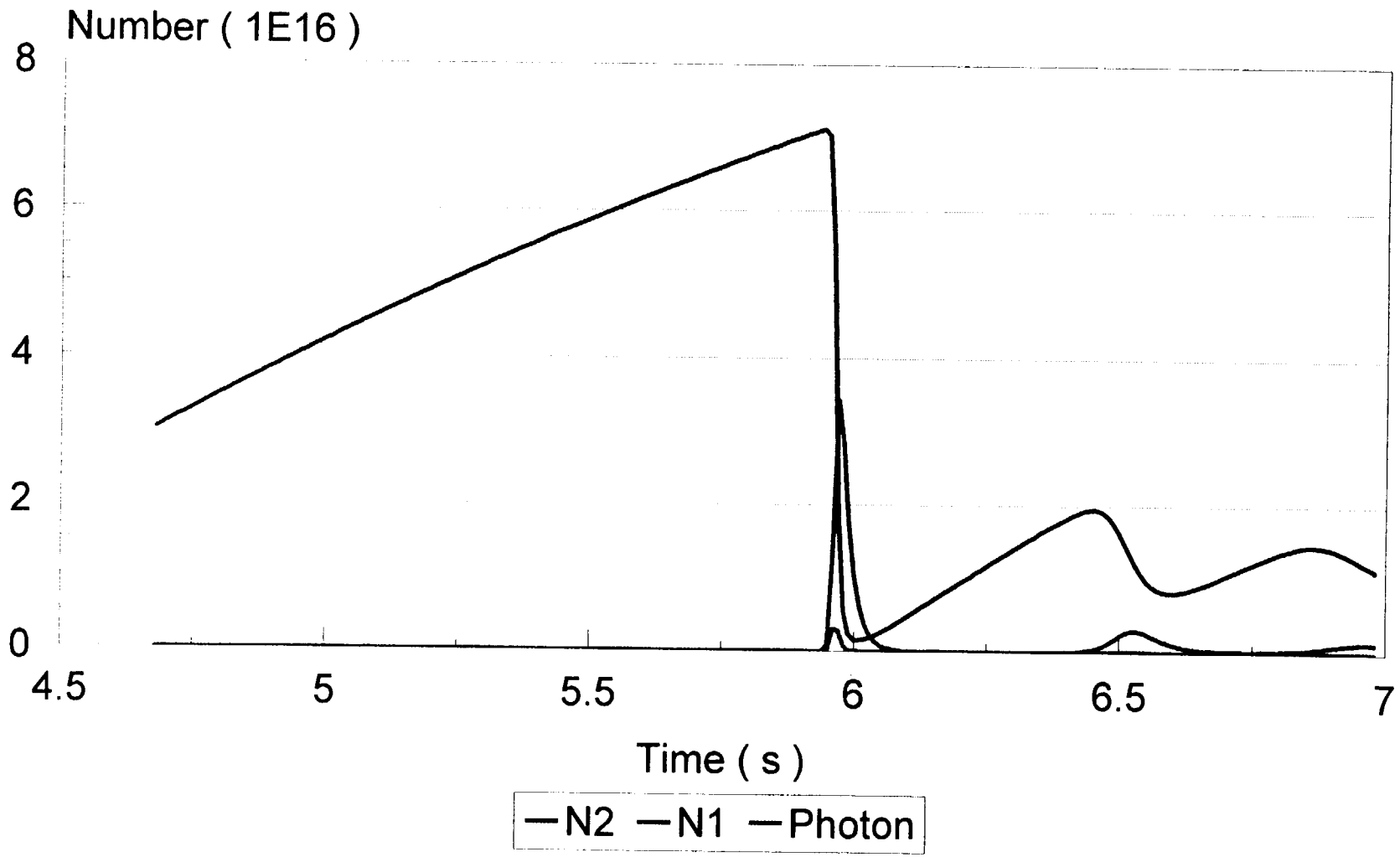

Figure 13. Output from the laser model with 140 J input Energy.

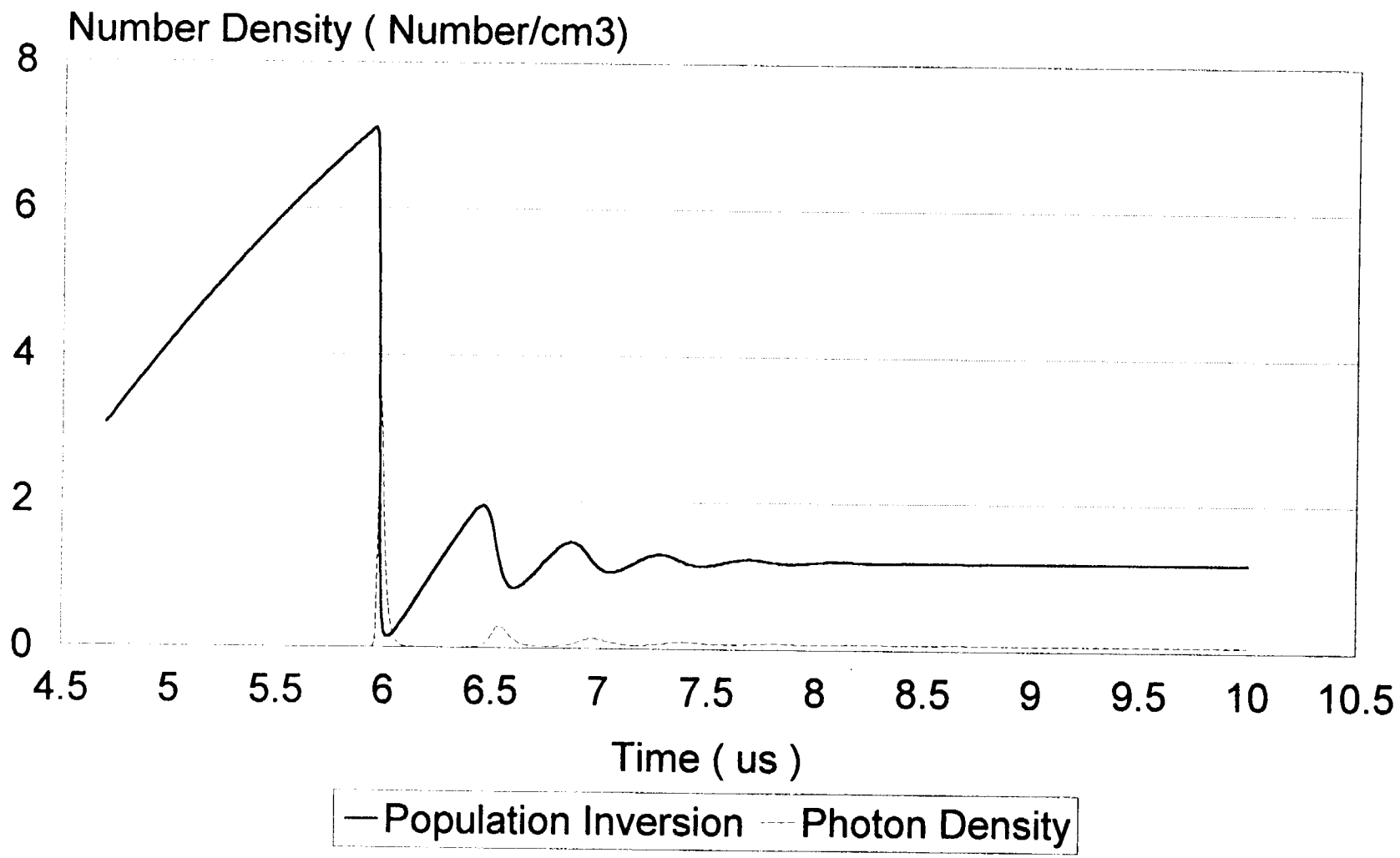

Figure 14 Output from the laser model with 80 J input Energy.